Journal of Asian Earth Sciences 35 (2009) 66–73

Contents lists available at ScienceDirect

Journal of Asian Earth Sciences

journal homepage: www.elsevier.com/locate/jaes

A comparative study of Dempster–Shafer and fuzzy models for landslide susceptibility mapping using a GIS: An experience from Zagros Mountains, SW Iran

Majid H. Tangestani *

Department of Earth Sciences, Faculty of Sciences, Shiraz University, 71454 Shiraz, Iran

ARTICLE INFO

Article history:
Received 16 April 2008
Received in revised form 21 December 2008
Accepted 5 January 2009

Keywords:
Landslide susceptibility
Hazard map
Dempster–Shafer
Fuzzy model
Iran

ABSTRACT

A catchment area at the Zagros Mountains, NW Shiraz, Iran is selected as a test site to comparing the output results of the Dempster–Shafer (D–S) and fuzzy models in landslide hazard mapping. Lithology, slope angle, slope aspect, land cover, and soil depth were considered as landslide causal factors. The factor maps were input into a GIS and a modified landslide hazard evaluation factor (MLHEF) rating and fuzzy membership functions as well as belief function values were assessed for each class of the factor maps. The fuzzy sum, product and gamma combination approaches were examined and output maps were assessed based on the known landslides. The outputs of fuzzy sum and product combination rules were not reasonable because these approaches classified the area into 'very-high' or 'very low' susceptibility zones respectively, which were not compatible to the field and factor maps criteria. A γ value of 0.94 yielded the most reliable susceptibility for landslides. Overlay of the known landslides with the output favorability map showed that the identified landslides were located in the high- and very-high susceptible zones. The output results of the Dempster–Shafer model: plausibility, belief, and uncertainty images were also evaluated based on the known landslides. The results of this approach revealed that although it was expected that most of the known landslides correspond the plausibility, or the belief map, only a few of them supported the case, and some landslides were coincided into the disbelief, or uncertainty maps. It is concluded that in comparison to the fuzzy model, the D–S model obtains less reliable results for landslide hazard mapping. Since the belief functions were assigned based on the fuzzy membership functions this might be due to the integration equations used by the model, or the number of evidence maps used as input layers.

1. Introduction

Landslides are naturally-occurring geologic processes that commonly cause different types of damages to people, landscapes, and constructions as well. They are defined as "abrupt, short-lived geomorphic events that constitute the rapid motion end of the mass movement spectrum" (Coates, 1977). Other terms used to denote this process are "landslip" and "mass-wasting", which include displacement of slopes forming earth material by fall, topple, slide or flow due to gravity (Varnes, 1978).

The assessment of landslide hazard and risk has recently become a topic of interest for both geoscientists and the local administrations (Carrara et al., 1991; Van Westen et al., 2000; Parise, 2001; Krejci et al., 2002; Demoulin and Chung, 2007; Nefeslioglu et al., 2008).

Many techniques have been proposed in literature for landslide hazard mapping (Hansen, 1984; Van Westen, 1993; Soeters and Van Westen, 1996). Van Westen et al. (1999) divided these techniques into two groups: 1- *Direct hazard mapping*, in which the degree of hazard is determined by the mapping geomorphologist, based on his experience and knowledge of the terrain condition; 2- *Indirect hazard mapping*, in which either statistical models or deterministic models are used to predict landslide prone areas, based on information obtained from the interrelation between landscape factors and the landslide distribution. With the increasing availability of high-resolution spatial data sets, GIS, remote sensing, and computers with large and fast processing capacity, it is becoming possible to partially automate the landslide hazard and susceptibility mapping process and thus minimize fieldwork (Temesgen et al., 2001; Van Lynden and Mantel, 2001; Gritzner et al., 2001; Ayalew and Yamagishi, 2005; Guinau et al., 2005; Fall et al., 2006; Zolfaghari and Heath, 2008; Yalcin, 2008). Quantitative prediction models for landslide hazard are based on a spatial database consisting of several layers of digital maps representing the casual factors for occurrence of landslides. Three mathematical frameworks used for the models are: (1) probability theory; (2) fuzzy set theory; and (3) Dempster–Shafer (D–S) evidential theory. Corresponding to the three theories, the "conditional probability function", the "fuzzy membership function", or the "belief

* Tel.: +98 711 6137222; fax: +98 711 2284572.
E-mail addresses: tangstan@shirazu.ac.ir, tangestani@susc.ac.ir

1367-9120/$ - see front matter © 2009 Elsevier Ltd. All rights reserved.
doi:10.1016/j.jseaes.2009.01.002

function" are used to represent a quantitative measure of future landslide hazard. These functions representing the landslide hazard were termed favorability functions. All models are based on two basic assumptions: (1) future landslides will occur under circumstances similar to those of past landslides in either the study area or in areas in which the experts have obtained their knowledge on the relationship between the causal factors and the occurrences of the landslides; and (2) the spatial data representing the causal factors contained in the GIS database can be used to formulate future landslides.

Several studies have used GIS and statistical models for landslide hazard and susceptibility mapping (Binaghi et al., 1998; Guzzetti et al., 1999; Sakellariou and Ferentinou, 2001; Gritzner et al., 2001; Ohlmacher and Davis, 2003; Gorsevski et al., 2006; Castellanos Abella and Van Westen, 2008), but mapping studies using fuzzy approach are limited (for example, Juang et al., 1992; Davis and Keller, 1997; Binaghi et al., 1998; Ercanoglu and Gokceoglu, 2002; Tangestani, 2004), and rare references are available applying Dempster–Shafer theory (Binaghi et al., 1998) . Using the appropriate causal factors and the efficient method for ranking importance of the factors and their internal classes (Donati and Turrini, 2002; Guzzetti et al., 1999) are also critical, and directly affect the quality of the output susceptibility maps.

This article focuses on comparing the output maps of the fuzzy and D–S models in assessing the landslide hazard based on the field criteria in the Kakan catchment area (Fig. 1), and includes four main steps: (1) producing the causal factors maps through studying aerial photographs and satellite images, field observations, and digital elevation processing; (2) evaluating the fuzzy membership and D–S belief functions for evidence maps using a modified method initially discussed by Anabalgan (1992); (3) using a GIS to produce the index maps and generating the resultant favorability, plausibility, and belief maps; and (4) comparing the output maps and controlling the reliability of them based on the previously mapped landslides.

2. Geology and geomorphology

Figs. 1 and 2 show the geomorphological features and the geology of the Kakan catchment area, respectively. This area is a mountainous terrain containing the northwesterly trending sedimentary rocks of the simply folded Zagros range. This area is part of the Kakan simple anticline trending northwest–southeast, with an inclination to the south, which starts from mid part of the area (Fig. 2). The youngest geological units are well-bedded Asmari–Jahrum Formation limestones of Oligocene–Miocene. This is a slightly weathered unit and forms the highest elevations in the area. The Cretaceous–Paleocene thin-bedded and highly weathered Pabdeh–Gurpi Formation underlies the Asmari Formation, and mostly comprises shale and marl. The Sarvak limestone, with an age of Upper Cretaceous, underlies the Pabdeh–Gurpi Formation. Colluvial and alluvial deposits, produced by the alteration processes of the exposed rocks, cover the foothills, piedmont slopes, and the Kakan plain as well. The stratigraphic contacts of geological units are conformable. A few normal faults with local importance occur in the middle parts of the Kakan anticline. However, some displacements in sedimentary beds of the southern area are due to a north–south striking fault (Fig. 2).

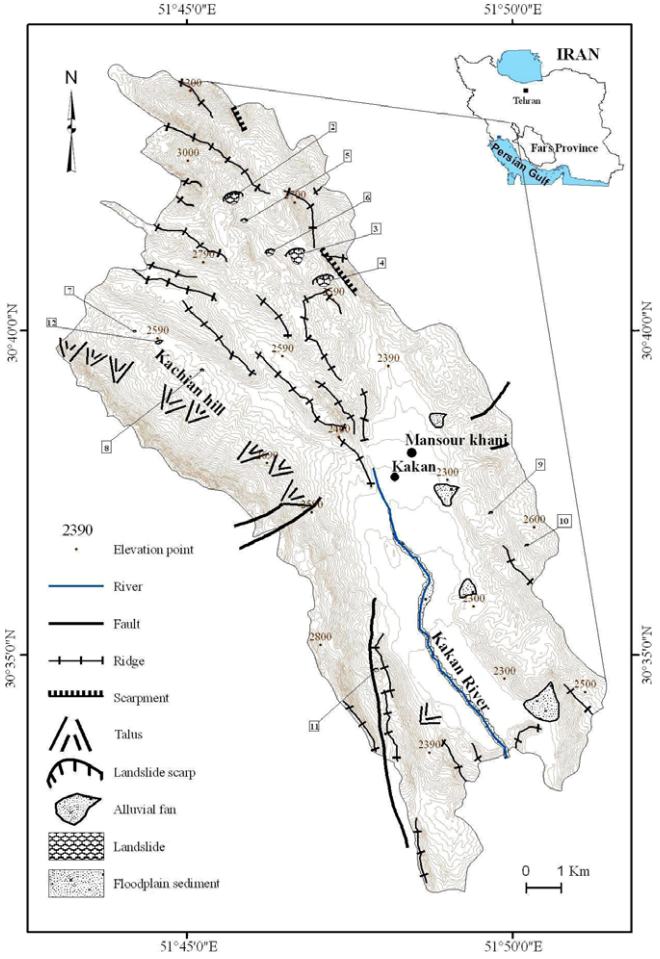

Fig. 1. Geographical location and geomorphology of the Kakan area.

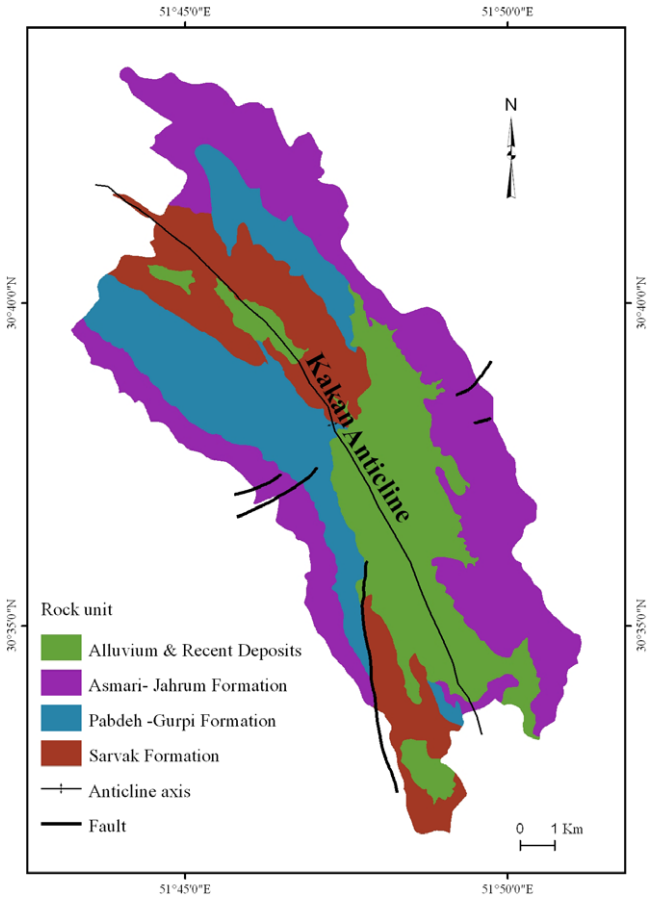

Fig. 2. Geological map of the study area.

The topography of the study area varies between 2200 and 3380 m, and the dominant range in elevation is 2400–2600 m. The higher elevations occur in the northwest. The drainage pattern is dendritic, and moderately irregular on the Pabdeh–Gurpi, and perpendicular to the common trend of the limestones of Asmari–Jahrum Formation. The main stream is the Kakan River, which flows from north to the south and is used for agricultural activities. There are also many subsidiary intermittent streams flowing only after rainy periods.

Most of the area (74%) is covered by pasture, 14% is utilized for agricultural activities and 1% for settlement purposes. Approximately 5% of the area contains rocky barren lands, and there is a sand quarry in the southern part of the catchment area. The mean annual precipitation of the area ranges 950–1200 mm, and the mean annual temperature is between 9 and 13 °C.

3. Landslide description

Landslides in the study area were identified from the interpretation of black and white aerial photographs at a scale of 1:40,000. There were 11 major landslides covering about 0.30 km^2 of the area (Fig. 1). Because of the low resolving power of the applied aerial photos the smaller landslides were not mapped. The mapped landslides were used for reliability control of the landslide hazard maps produced by the fuzzy and D–S belief models.

Although a variety of small-scale mass wasting is observed during the field studies, the area is primarily affected by the slope movements due to the precipitations in rainy seasons. The smallest landslide identified from the aerial photographs and subsequently recognized in the field has an extent of 2403 m^2 (No. 10 in Fig. 1) while the largest one, located in the northern part of area, is 93,120 m^2 (No. 3 in Fig. 1). Landslide classification systems are commonly based on a combination of material and movement mechanism. Using the system proposed by Cruden and Varnes (1996), the mapped landslides of the study area are shallow-seated debris slides or complex debris slide-flows, and generally are suspended-dormant. The materials involved in landslides are a mixture of soils, gravels and cobbles. Considering the geological and the climatic characteristics of the region, the main landslide triggering factor in the area is rainfalls.

Field checking indicated that the three failures in Asmari–Jahrum and Sarvak Formations were debris slides occurred in the colluvium, and that the failure mode was of the translational type, involving a slipping of a layer of colluvium. Other 8 landslides occurring in shaly-marly Pabdeh–Gurpi Formation were rotational type debris slides or complex debris slide-flows. The sliding bodies commonly originated from fine-grained shaly-marly deposits accumulated on the hill slopes. These types of landslides generally started as slides, but were consequently converted to flows because of the water involved and the steep terrain below the landslide sources. The main scarps of the landslides vary between 0.5 and 3.0 m with a mean value of about 1.5 m.

4. Fuzzy and Dempster–Shafer models

When producing landslide hazard maps, some researchers have employed quantitative methods (Carrara et al., 1991; Anabalgan, 1992; Juang et al., 1992; van Westen et al., 1997; Guzzetti et al., 1999; Gritzner et al., 2001; Ercanoglu and Gokceoglu, 2002). All the available methods for regional landslide assessment have some uncertainties arising from lack of knowledge and variability. This is because regional landslide assessments require some generalizations and simplifications, although these assessments are complex. For this reason, a perfect assessment method for landslide susceptibility does not exist. The fuzzy and Dempster–Shafer models, which are implemented in this paper, are briefly described below.

4.1. Fuzzy model

The idea of fuzzy logic (Zadeh, 1965) is to consider the spatial objects on a map as members of a set. In classical set theory, an object is a member of a set if it has a membership value of 1, or not a member if it has a membership value of 0. In fuzzy set theory, membership can take on any value between 0 and 1 reflecting the degree of certainty of membership. Fuzzy set theory employs the idea of a membership function that expresses the degree of membership with respect to some attribute of interest. Working in GIS with map layers, generally the attribute of interest is measured over discrete intervals, and the membership function can be expressed as a table relating map classes to membership values. Fuzzy logic is attractive because it is straightforward to understand and implement. It can be used with data from any measurement scale and the weighting of evidence is controlled by the expert. Fuzzy logic method allows for more flexible combinations of weighted maps, and can be readily implemented with a GIS modeling language.

When using fuzzy logic in landslide susceptibility mapping the spatial objects on a map are considered as members of a set. For example, the spatial objects could be areas on an evidence map (map of causative factors for land sliding) and the set defined as "areas susceptible to landslide".

A variety of operators can be employed to combine the membership values when two or more maps with fuzzy membership functions for the same set are available. An et al. (1991) discussed five operators, namely the fuzzy AND, fuzzy OR, fuzzy algebraic product, fuzzy algebraic sum and fuzzy gamma operator. This study uses the fuzzy algebraic sum, the fuzzy algebraic product, and fuzzy gamma operator for combining the fuzzy membership functions.

4.2. Dempster–Shafer theory of evidence

Dempster–Shafer Theory (DST) (Dempster, 1967; Shafer, 1976) is a mathematical theory of evidence which is used to combine separate pieces of information (evidence) to calculate the probability of an event. When applied to a body of evidence, the DST has domain-independent inference capability in combining evidence and, in the process, representing some levels of ignorance. In DS theory, a problem domain is represented by a finite set Θ of mutually exclusive and exhaustive hypotheses, called *frame of discernment*. In the standard probability framework, all elements in Θ are assigned a probability; and when the degree of support for an event is known, the remainder of the support is automatically assigned to the negation of the event. On the other hand, in DS theory, basic probability assignments are carried out for events, and committing support for an event does not necessarily imply that the remaining support is committed to its negation. The frame of discernment, and the three important functions in Dempster–Shafer theory: the *basic probability assignment*, or *mass* function (bpa or *m*), the *Belief* function (*Bel*), and the *Plausibility* function (*Pl*), as well as the combination rules implemented in this paper are described in the following subsections.

4.2.1. Frame of discernment

Suppose an interpreter needs to analyze a satellite image of an agricultural site. To his knowledge, this area contains only two summer crops: cotton (cn) and sunflower (sf); and two winter crops: wheat (wh) and pea (pe). The set of possible hypotheses, which is called a Frame of Discernment (FoD) is defined as: Θ = (cn, sf, wh, pe), in which each compatible possibility (crop type)

in Θ is called a singleton. Since the hypotheses in Θ are exhaustive the empty set, Φ is considered as a false hypothesis in Θ. DST enables us to consider not only single classes, but also groups of classes, such as summer crops, i.e., (cn, sf) in our example. The set of all subsets of Θ is denoted 2^{Θ}, and a set of size n has $2^n - 1$ true hypotheses.

4.2.2. Basic probability assignment

Suppose that there is a body of evidence in support of the non-empty subset A of 2^{Θ}. A function $m(A)$, called the Basic Probability Assignment (BPA), assigns to hypothesis A, a degree, denoted m, to which the evidence supports the hypothesis. The degrees of support are numbers in the range of [0,1] and must sum to 1 over all possible hypotheses (Eq. (1)):

$$m : \left\{ \sum_{A \in 2\Theta}^{m(\Theta)=0} m(A) = 1 \right. \quad (1)$$

when, A$\in 2^{\Theta}$, the quantity $m(A)$ is the belief committed to A.

4.2.3. Belief and plausibility functions

From the basic probability assignment, the upper and lower bounds of an interval can be defined. This interval contains the precise probability of a set of interest and is bounded by two non-additive continuous measures called Belief and Plausibility. The lower bound *Belief* for a set A is defined as the sum of all the basic probability assignments of the proper subsets (B) of the set of interest (A) ($A \subset B$). The upper bound, *Plausibility*, is the sum of all the basic probability assignments of the sets (B) that intersect the set of interest (A) ($A \cap B \neq \emptyset$) .

4.2.4. Combination of belief functions

Evidences from two or more maps are combined using Dempster's rule of combination (Wright and Bonham-Carter, 1996). The combined belief, plausibility, disbelief, and uncertainty can each be separately mapped, although only two of these quantities are independent.

Each map to be used as evidence to evaluate a proposition is associated with a pair of belief functions (support function and the plausibility function). In practice, these functions are usually held in map attribute tables, where each class on the map is associated with a support value and a plausibility value. Suppose we have map A, we will simply denote the value of the support due to A, as Sup_A, and the plausibility due to A, as Pls_A. Because functions vary with the value (map class) of A, they can therefore be mapped in their own right by lookup operations from map A. For a given value of map A, the uncertainty is denoted as Unc_A, calculated as Pls_A-Sup_A, and the disbelief, Dis_A, is 1-Pls_A. Thus the sum $Sup_A + Unc_A + Dis_A = 1$. The disbelief is the belief that the proposition is false, i.e., that a cell does not contain a landslide.

Given two maps A and B, with the support and disbelief functions for each, Dempster's rule of combination for estimating the combined support, disbelief and uncertainty are shown in Eqs. (2)–(4) (Wright and Bonham-Carter, 1996). The Dempster rule of combination is purely a conjunctive operation (AND). The combination rule results in a belief function based on conjunctive pooled evidence (Shafer, 1986).

$$Spt_C = \frac{Spt_A Spt_B + Spt_A Unc_B + Spt_B Unc_A}{\beta} \quad (2)$$

$$Dis_C = \frac{Dis_A Dis_B + Dis_A Unc_B + Dis_B Unc_A}{\beta} \quad (3)$$

$$Unc_C = \frac{Unc_A Unc_B}{\beta} \quad (4)$$

where, the denominator for all three equations is calculated using Eq. (5).

$$\beta = 1 - Spt_A Dis_B - Dis_A Spt_B \quad (5)$$

The term β is a normalizing factor that ensures that Spt + Dis + Unc = 1. More information on the Dempster–Shafer Theory could be found in Shafer (1990).

5. Evidence maps

The primary causal factors for landslide hazard mapping in the study area include slope angle, slope aspect, lithology, land use, and soil depth, produced from topographical data processing, satellite images and aerial photographs interpretation, and the field surveys as well. The generated evidence maps were processed and analyzed in ArcGIS, Arcview, and IDRISI software packages. All the data layers were geo-referenced in the Universal Transverse Mercator (UTM) geographic reference system. The basic probabilities in DS theory (degree of belief and the degree of plausibility) and the weighting scores (membership functions) in fuzzy model were evaluated and assigned to map classes subjectively. This is a knowledge-driven method generally applicable in areas where landslides are either unknown, or low information is available regarding the occurrence of them.

In fuzzy model, the spatial objects on each map were evaluated according to the proposition "susceptible locations to land sliding", and fuzzy membership functions were assigned to each map layer which was used as evidence in support of this proposition. In D–S belief model, the Belief and Plausibility functions of causal factor maps were assigned based on the weight of fuzzy membership function in each class to give similar subjective function to each map class (Table 1). The fuzzy membership values were chosen based on subjective judgment about the relative importance of the map classes. Anabalgan (1992) proposed a numerical rating scheme based on an empirical approach for the landslide causative factors including geology, slope morphometry, relative relief, land use and land cover and groundwater conditions. He assigned the maximum rating of 2 or 1 for a variety of subcategories of each causative factor (Anabalgan, 1992, Table 2). Since most of the factors introduced by Anabalgan were inherently causative for slope instability at the area and because of the similarities of subcategories, a modified rating scheme was proposed for the study area. Weighting rates based on the author's knowledge were evaluated and assigned to factor map classes in a way that each class on the map had a value between 0 and 1 (Table 1).

The geological units were reclassified into two rock types due to their relationship to the landslide susceptibility; limestone and the shaly-marly exposures. The Quaternary alluvial deposits cover the remaining Kakan catchment area. Ratings of rock types based on Anabalgan (1992) were assigned to each class and the fuzzy membership functions were evaluated based on the expert knowledge. Since the higher plausibility and belief functions are logically correspondent with the higher fuzzy membership functions the D–S belief functions were then evaluated subjectively based on the fuzzy membership functions (Table 1).

The soil map was produced from the laboratory results of 50 soil profiles. The depth and texture of soil types were considered when evaluating ratings and fuzzy membership functions based on the rating scheme suggested by Anabalgan (1992). The rock types and the soil types covering the Quaternary alluvial deposits were combined in a single data layer, and the fuzzy membership functions were assigned for each map class (Table 1). The soil depth map was also generated by the use of soil profiles data. The ratings and fuzzy membership as well as D–S belief functions of each map class were evaluated using the ratings suggested by Anabalgan (1992).

Table 1
LHEF ratings, fuzzy membership functions, and the D–S belief functions assigned for factors classes.

Class No.	Lithology	LHEF rating	Fuzzy	Belief	Plausibility
1	Limestone	0.2	0.1	0.10	0.80
2	Older alluvial deposits	0.8	0.4	0.15	0.82
3	Clayey soil	1.0	0.5	0.20	0.85
4	Shale and marl	2.0	1.0	0.25	0.95
5	Younger terraces and alluvium	2.0	1.0	0.25	0.95
Soil depth					
1	<5 m	0.65	0.25	0.10	0.70
2	6–10 m	0.85	0.4	0.18	0.82
3	11–15 m	1.30	0.65	0.22	0.90
4	16–20 m	2.0	1.0	0.25	0.95
5	>20 m	1.20	0.6	0.20	0.85
Slope angle (°)					
1	<15	0.5	0.2	0.15	0.82
2	15–25	0.8	0.4	0.18	0.83
3	25–35	1.2	0.6	0.20	0.85
4	35–45	1.7	0.9	0.22	0.92
5	>45	2.0	1.0	0.25	0.95
Slope aspect					
1	North-facing	2.0	1.0	0.20	0.92
2	South-facing	0.6	0.3	0.12	0.83
3	East-facing	1.0	0.5	0.15	0.85
4	West-facing	1.6	0.8	0.18	0.90
5	plains	0.2	0.1	0.10	0.80
Land cover					
1	Agricultural land (21,22)	0.6	0.3	0.10	0.83
2	Thickly vegetated area	0.80	0.4	0.15	0.85
3	Moderately vegetated area	1.4	0.7	0.20	0.90
4	Sparsely vegetated area	2.6	1.0	0.25	0.95
5	Barren land	0.4	0.2	0.05	0.82

Table 2
Landslide susceptibility zonation on the basis of output fuzzy membership functions.

Zone	Fuzzy membership function	Description
I	<0.1	Non-susceptible zone
II	0.1–0.4	Low susceptible zone
III	0.4–0.6	Moderate susceptible zone
IV	0.6–0.75	High susceptible zone
V	>0.75	Very high susceptible zone

The slope angle map was produced automatically in IDRISI using the digital elevation model (DEM) of topographical data at a scale of 1:25,000, with contour intervals of 20 m, and a 25 m× 25 m grid size. Anabalgan (1992) introduces a subjective scheme for slope angle rating. The area has slope angles varying in the range 0°–70°. However, slopes of more than 45° occur mostly on Asmari Formation limestone. Table 1 shows the slope angle classes and the fuzzy membership and D–S belief functions assigned to each map class.

The slope aspect map for five main slope directions was also produced from the DEM. In fact the slope aspect is mostly related to the physiographic trends and/or the receiving precipitation due to the prevailing winds (Ercanoglu and Gokceoglu, 2002). It is observed that the northern- and western-facing slopes retain higher moisture content in a longer time, causing higher landslide susceptibility. The fuzzy membership and D–S belief functions for different slope directions were evaluated based on the fact that the northern- and western-facing aspects have an increase sliding susceptibility (Table 1).

Land cover acts as a protection and reduces the susceptibility of soil erosion, landslides and the splash action of the rainwater. Aerial photographs and Landsat ETM$^+$ data interpretation along with field observations were used to delineate the land cover types in the area. Five classes of land use were identified: sparsely vegetated area (60%), moderately vegetated area (14%), thickly vegetated area (1%), agricultural lands (19%), and barren lands, including rocky exposures, urban areas, and river bed (6%). Although Anabalgan (1992) assigns the highest rating to the barren lands, field observations at the study area showed that these areas were mostly the limestone units with low susceptibility to landslides. This leds to a modified fuzzy membership functions, which were evaluated on the basis of modified ratings. The D–S belief functions were then evaluated based on the fuzzy membership functions (Table 1).

6. Results and discussion

The input layers were processed after fuzzy membership and D–S belief functions were assigned for each map class. The rock and soil types were combined to generate the lithology factor map showing the same importance for the two evidences. Five primary causal factors including lithology, land cover, slope aspect, slope angle, and soil depth were integrated to generate the final output maps using fuzzy sum, product, and gamma operators, and the combination rules of Dempster–Shafer model as well.

In Dempster–Shafer model, the belief functions assigned to each map class was used by the system for generating the output Belief, Plausibility, and Uncertainty maps.

The classification scheme suggested by Anabalgan (1992) was used for landslide hazard zonation in the study area, based on the fuzzy model (Table 2). The Belief, Plausibility and Uncertainty output maps produced by the Dempster–Shafer model were reclassified in function intervals of 0.1, 0.1, and 0.05, respectively.

The fuzzy sum, and product combination rules were run on 5 main causal factor maps, and each output layer was classified according to the intervals of 0.1 for membership function. The known landslides were then overlaid the landslide susceptibility maps to examine the degree of coincidence of susceptibility with land sliding. The fuzzy sum operation evaluated the land sliding susceptibility of the area in range of 0.60–1.00. When the output map was reclassified into 0.1 intervals, more than 96% of pixels were in range of 0.90–1.00, 2.76% in range of 0.80–0.90, and 0.92% in range of 0.70–0.80, and only 4 pixels were in range of 0.60–0.70. Overlay of reclassified fuzzy sum output image and known landslides showed that all the 111 pixels of known landslides were located in the susceptibility range of 0.90–1.00. On the other hand, the output susceptibility map based on the fuzzy product operation generated a maximum membership function of 0.143. This low value is due to the decreasing effect of fuzzy product operation. This operation results in coincidence of known landslides with non-susceptible and low-susceptible zones, which could not be a reasonable result. γ values of 0.90, 0.92, and 0.94 were tested on the input fuzzy data layers and the results were compared using the known landslides as the criteria for validation (Table 3). As is evident from Table 3 γ value of 0.90 classifies about 64% of pixels of the area in "high- and very-high susceptible" zones. 96 pixels of known landslides were located in "high susceptible" zone and 14 pixels in very-high susceptible zone. γ values of 0.92 and 0.94 accumulated about 91 and 96% of the area in susceptibility classes 4 and 5, respectively. Coincidence of 78 and 109 pixels of known landslides into "very-high susceptible" zone verifies that increment of the γ values increases the susceptibility of the study area to land sliding and result in coincidence of more known landslides on the higher susceptible zones. The output susceptibility map generated based on fuzzy γ value of 0.94 is shown in Fig. 3. Susceptible zones with fuzzy membership functions more than 0.75 were mostly coincident into the shaly-marly rock units of the Pabdeh–Gurpi Formation. Tangestani (2004) suggested that

Table 3
The results of performing fuzzy gamma approach, in case of assigning three values for γ, and the degree of coincidence of known landslides with susceptibility classes.

Susceptibility class	Fuzzy membership function	γ = 0.90Class pixels	γ = 0.90 Known slides	γ = 0.92 Class pixels	γ = 0.92 Known slides	γ = 0.94 Class pixels	γ = 0.94 Known slides
Non-susceptible	<0.1	0	0	0	0	0	0
Low susceptibility	0.1–0.4	595(1.31%)	0	8(0.02%)	0	0	0
Moderate susceptibility	0.4–0.6	15,312 (33.54%)	1	3846 (8.42%)	0	1559 (3.42%)	0
High susceptibility	0.6–0.75	24,482 (53.62%)	96	32,279 (70.7%)	33	20,793 (45.54%)	2
Very high susceptibility	>0.75	5266 (11.53%)	14	9522 (20.86%)	78	23,303 (51.04%)	109

assigning a value of 0.6 for γ in the same area decreased the fuzzy membership functions in output map to <0.3, which is coincided only with "low-susceptibility" zones.

The BELIEF decision support module in IDRISI software was used in generating the belief output images including Belief (or Support), Plausibility, and "Belief interval" or Uncertainty. The results were then compared to the known landslides to evaluate the degree of coincidence (Table 4). The output Belief or Support image (Fig. 4) represents the degree to which the evidence provides concrete support for the proposition of land sliding. The belief image classifies the study area in four main intervals, ranging 0.10–0.45. About 73% of the area reveals the support interval of 0.10–0.30, in which all the 111 pixels of known landslides were located. Although more than 27% of the area showed the belief function of more than 0.30, none of the mapped landslides coincided with this level of support. Weak support is found in both areas

Table 4
The statistical results of Belief, Uncertainty, and Plausibility output images, and the degree of coincidence of known landslides with susceptibility classes.

Belief Class No.	Belief interval	Pixels in class	Percent in area	Pixels of known landslides
1	0.10–0.20	8306	18.19	42
2	0.20–0.30	24,971	54.68	69
3	0.30–0.40	11,055	24.20	0
4	0.40–0.50	1340	2.93	0
Uncertainty Class No.	Uncertainty interval			
1	0.20–0.25	45,542	99.71	111
2	0.25–0.30	133	0.29	0
Plausibility Class No.	Plausibility interval			
1	0.30–0.40	6911	15.13	42
2	0.40–0.50	20,731	45.38	68
3	0.50–0.60	15,651	34.27	1
4	0.60–0.70	2382	5.22	0

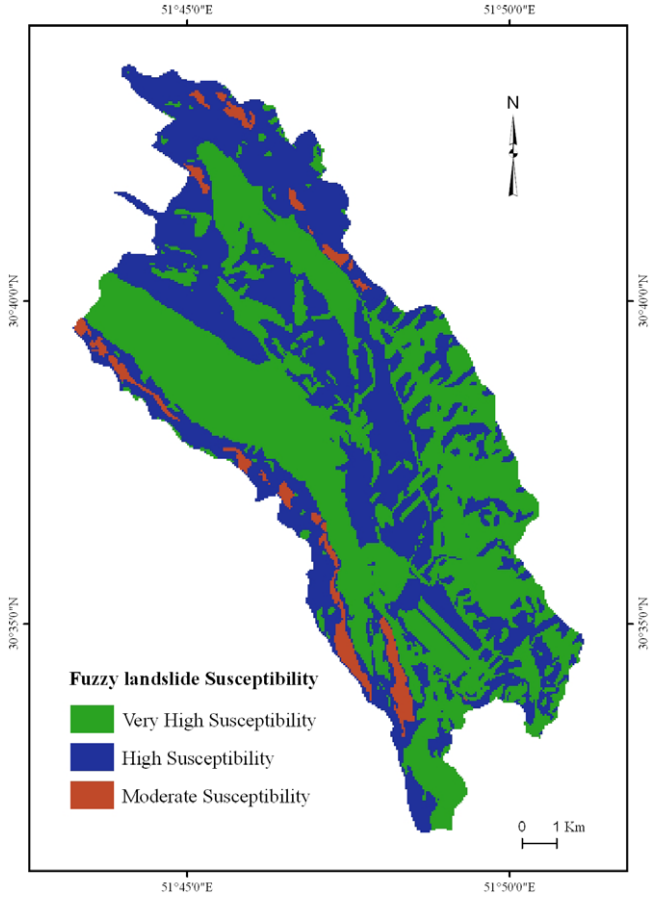

Fig. 3. Landslide hazard map generated by fuzzy gamma approach, in case of value 0.94 for γ.

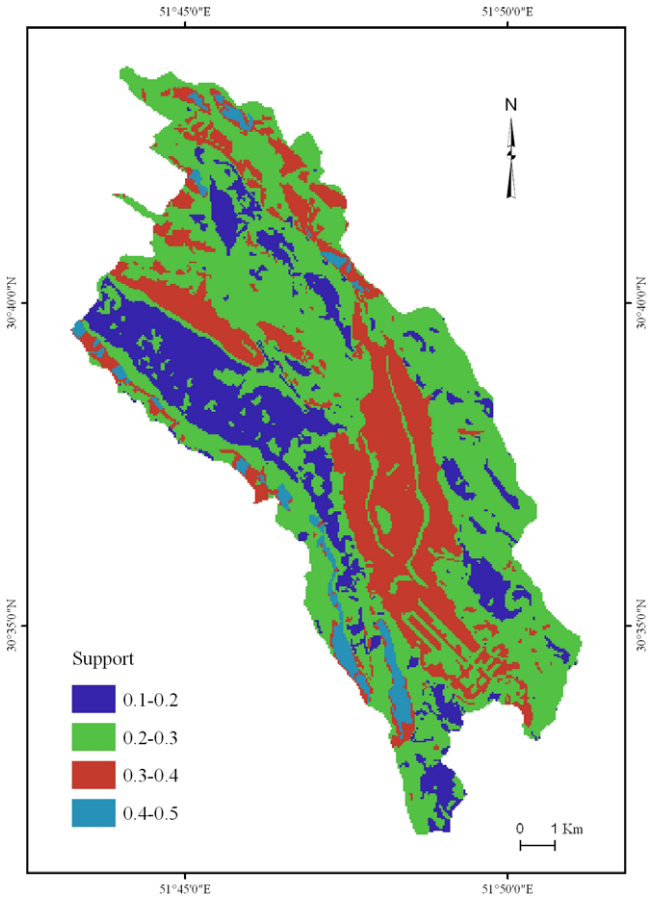

Fig. 4. Support image generated by the use of D–S combination rules.

where the data sets provide weak support for the target proposition and where there are fewer spatial data layers. The plausibility image (Fig. 5) shows the degree to which the evidence does not refute the proposition. It is expected that most known landslides coincide into the highest levels of plausibility. The study area shows plausibility in a range of 0.30–0.67, being reclassified into intervals of 0.10. More than 45% of pixels were located in a range of 0.40–0.50, and 34% in an interval of 0.50–0.60. Overlay of known landslides on the plausibility image revealed that 42 pixels were located in a plausibility range of 0.30–0.40 and 68 pixels in interval of 0.40–0.50. Only one pixel was located on the areas with plausibility of more than 0.50. Uncertainty is the difference between plausibility and support and acts as a measure of uncertainty about a proposition. The uncertainty image collected about 99.71% of the area in values of 0.20–0.25, and 0.29% in uncertainty of 0.25–0.30. Although the highest level of uncertainty does not exceed the value of 0.30, all the 111 pixels of known landslides were located in the interval of 0.20–0.25.

Discrepancies between the D–S theory output results and the known criteria arise mainly from the combination rules proposed by the theory (Xu et al., 1992; Al-Ani and Deriche, 2002; Yamada, 2008). Attractive features of the combining function are: 1. Concordant items of evidence reinforce each other; 2. Conflicting items of evidence erode each other. In the opposite situation, when evidential rules differ substantially in their conclusions, the combining rule of D–S theory may produce answers that disagree with the evidence (Murphy, 2000). Therefore, the degree of conflict of the sources must always be taken into account before taking a final decision based on the Dempster's rule to minimizing the decision errors generated by the fusion process (Zadeh, 1979). In the case of landslide hazard mapping conflicts may arise in areas where landslide-prone rock units such as marl and shale or deep soils locate in gentle slopes, or steep slopes are geologically containing limestone or dolomite. Some work has been done to improve the efficiency of the Dempster–Shafer method using different approaches (for example: Josang, 2002; Lefevre et al., 2002; Murphy, 2000).

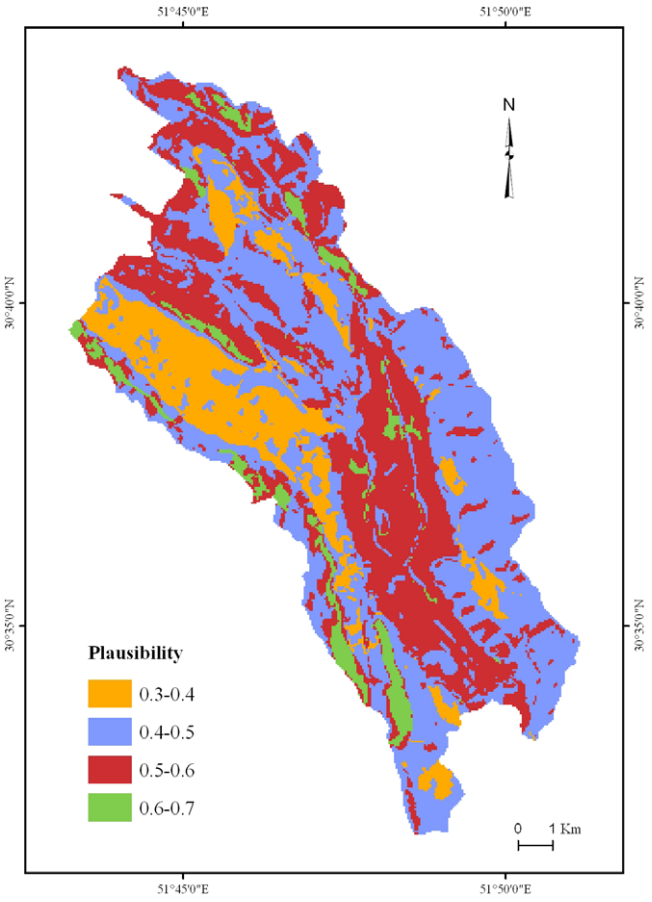

Fig. 5. Plausibility image generated by the use of D–S combination rules.

7. Conclusion

Two GIS-based methodologies for landslide hazard mapping were tested in a landslide prone area, SW Iran, and the outputs were compared. The gamma fuzzy logic approach used in this paper provides a flexible method with which to include an expert's opinion in developing an inference network, while the Dempster–Shafer belief model uses the combination rules in which the expert only can assign the belief functions for each factor map class. Integration of fuzzy and D–S combination rules and GIS facilities enables the expert to examine different scenarios, and to add any new data layer to the model and test its effect on the final susceptibility map.

The fuzzy algebraic sum classifies more than 96% of the area in fuzzy membership functions in a range of 0.90–0.10, meaning that nearly all the area is very susceptible to land sliding. The fuzzy algebraic product, on the other hand, classifies the area into fuzzy membership functions <0.143, which coincides into the category of "low-susceptibility" for land sliding. It is clear from the geology of the area, other causal factors and the field evidences that none of the results is reasonable, and that these two fuzzy combination rules are rejected in order to be used for landslide hazard mapping. The mathematical relations presented for the fuzzy sum and product operators are responsible for these types of discrepancies.

Because of the ease with which the fuzzy gamma value can be edited with a GIS system, it is easy to try various scenarios to improve the match with known landslides or minimize the effects of overestimated membership values. The effects of choosing different values for γ (between 0 and 1) are discussed by Bonham-Carter (1994). γ values assigned for each γ combination operation play the most important role on the output membership functions. Owing to the constant value for γ, the outputs are essentially based on the fuzzy membership functions assessed with respect to factor maps classes. Choosing a γ value of 0.94 for this study reflects the expert's opinion for giving an increasive possibility value to the final map. Because of the correspondence of areas with higher susceptibility into the known landslides this could be an acceptable result for a medium-scale landslide susceptibility map. The use of fuzzy gamma operation in the generation of the landslide susceptibility map seems to be a reliable approach.

Results obtained by the models were mostly dependent on data quality, the fuzzy membership and D–S belief functions assigned to each evidence map class, the γ values employed in the fuzzy combination model, and the D–S combination rules for generating the belief images. Comparison of fuzzy output susceptibility map and the plausibility image of D–S model with the field criteria collected in the known landslides map revealed that the fuzzy gamma approach with a value of 0.94 for γ gives more reasonable results. Since the D–S belief functions assigned to the factor map classes were based on the fuzzy membership functions, it is concluded that less compatibility of the plausibility image to the known landslides was primarily due to a degree of conflict between evidence factors and the limitations in combination rules used by the belief model.

Acknowledgements

This research was in part supported by the research funds of the Shiraz University, Shiraz, Iran. The author would like to thank the 3

unnamed reviewers for their informative and constructive comments.

References

Al-Ani, A., Deriche, M., 2002. A new technique for combining multiple classifiers using the Dempster–Shafer theory of evidence. Journal of Artificial Intelligence Research 17, 333–361.

An, P., Moon, W.M., Rencz, A., 1991. Application of fuzzy set theory for integration of geological, geophysical, and remote sensing data. Canadian Journal of Exploration Geophysics 27, 1–11.

Anabalgan, R., 1992. Landslide hazard evaluation and zonation mapping in mountainous terrain. Engineering Geology 32, 269–277.

Ayalew, L., Yamagishi, H., 2005. The application of GIS-based logistic regression for landslide susceptibility mapping in the Kakuda-Yahiko Mountains, Central Japan. Geomorphology 65, 15–31.

Binaghi, E., Luzi, L., Madella, P., Rampini, A., 1998. Slope instability zonation: a comparison between certainty factor and fuzzy Dempster–Shafer approaches. Natural Hazards 17, 77–97.

Bonham-Carter, G.F., 1994. Geographic Information Systems for Geoscientists: Modelling with GIS. Springer. p. 393.

Carrara, A., Cardinali, M., Detti, R., Guzzetti, F., Pasqui, V., Reichenbach, P., 1991. GIS techniques and statistical models in evaluating landslide hazard. Earth Surface Processes and Landforms 16, 427–445.

Castellanos Abella, E.A., Van Westen, E.A., 2008. Qualitative landslide susceptibility assessment by multicriteria analysis: A case study from San Antonio del Sur, Guantánamo, Cuba. Geomorphology 94, 453–466.

Coates, D.R., 1977. Landslide perspectives. In: Coates, D.R. (Ed.), Landslides, Reviews in Engineering Geology, vol. 3. Geological Society of America, Boulder, Colarado, pp. 3–28.

Cruden, D.M., Varnes, D.J., 1996. Landslide types and processes. In: Turner, A.K., Schuster, R.L. (Eds.), Landslides: Investigation and Mitigation. National Academy Press, Washington, DC, pp. 36–75.

Davis, T.J., Keller, C.P., 1997. Modelling uncertainty in natural resource analysis using fuzzy sets and Monte Carlo simulation: slope stability prediction. International Journal of Geographical Information Systems 11 (5), 409–434.

Dempster, A.P., 1967. A generalization of Bayesian inference. Journal of Royal Statistics Society 30, 205–247.

Demoulin, A., Chung, C.F., 2007. Mapping landslide susceptibility from small datasets: a case study in the Pays de Herve (E Belgium). Geomorphology 89, 391–404.

Donati, L., Turrini, M.C., 2002. An objective method to rank the importance of the factors predisposing to landslides with the GIS methodology: application to an area of the Apennines (Valnerina; Perugia, Italy). Engineering Geology 63, 277–289.

Ercanoglu, M., Gokceoglu, C., 2002. Assessment of landslide susceptibility for a landslide-prone area (north of Ynice, NW Turkey) by fuzzy approach. Environmental Geology 41, 720–730.

Fall, M., Azzam, R., Noubactep, C., 2006. A multi-method approach to study the stability of natural slopes and landslide susceptibility mapping. Engineering Geology 82, 241–263.

Gorsevski, P.V., Gessler, P.E., Boll, J., Elliot, W.J., Foltz, R.B., 2006. Spatially and temporally distributed modeling of landslide susceptibility. Geomorphology 80, 178–198.

Gritzner, M.L., Marcus, W.A., Aspinall, R., Custer, S.G., 2001. Assessing landslide potential using GIS, soil wetness modelling and topographic attributes, Payetti River, Idaho. Geomorphology 37, 149–165.

Guinau, M., Palla's, R., Vilaplana, J.M., 2005. A feasible methodology for landslide susceptibility assessment in developing countries: a case-study of NW Nicaragua after Hurricane Mitch. Engineering Geology 80, 316–327.

Guzzetti, F., Carrara, A., Cardinali, M., Reichenbach, P., 1999. Landslide hazard evaluation: a review of current techniques and their application in a multi-scale study, Central Italy. Geomorphology 31, 181–216.

Hansen, A., 1984. Landslide hazard analysis. In: Brunsden, D., Prior, D.B. (Eds.), Slope Instability. Wiley & Sons, New York, pp. 523–602.

Josang, A., 2002. The consensus operator for combining beliefs. Artificial Intelligence 141, 157–170.

Juang, C.H., Lee, D.H., Sheu, C., 1992. Mapping slope failure potential using fuzzy sets. Journal of Geotechnical Engineering ASCE 118 (3), 475–493.

Krejci, O., Baron, I., Bil, M., Hubatka, F., Jurova, Z., Kirchner, K., 2002. Slope movements in the Flysch Carpathians of Eastern Czech Republic triggered by extreme rainfalls in 1997: a case study. Physics and Chemistry of the Earth, Parts A/B/C 27 (36), 1567–1576.

Lefevre, E., Colot, O., Vannoorenberghe, P., 2002. Belief function combination and conflict management, Inform. Fusion 3, 149–162.

Murphy, C.K., 2000. Combining belief functions when evidence conflicts. Decision Support Systems 29, 1–9.

Nefeslioglu, H.A., Duman, T.Y., Durma, S., 2008. Landslide susceptibility mapping for a part of tectonic Kelkit Valley (Eastern Black Sea region of Turkey). Geomorphology 94, 401–418.

Ohlmacher, G.C., Davis, J.C., 2003. Using multiple logistic regression and technology to predict landslide hazard in northeast Kansas, USA. Engineering Geology 69, 331–343.

Parise, M., 2001. Landslide mapping techniques and their use in the assessment of the landslide hazard, Physics and chemistry of the Earth, Part C. SolarTerrestrial & Planetary Science 26 (9), 697–703.

Sakellariou, M.G., Ferentinou, M.D., 2001. GIS-based estimation of slope stability. Natural Hazards Review 2 (1), 12–21.

Shafer, G., 1976. A Mathematical Theory of Evidence. Princeton University Press, New Jersey.

Shafer, G., 1986. Probability judgement in artificial intelligence. In: Kanal, L.N., Lemmer, J.F. (Eds.), Uncertainty in Artificial Intelligence. Elsevier Science, New York.

Shafer, G., 1990. Perspectives on the theory and practice of belief functions. International Journal of Approximate Reasoning 3, 1–40.

Soeters, R., Van Westen, C.J., 1996. Slope instability recognition, analysis, and zonation. In: Turner, A.K., Schuster, R.L. (Eds.), Landslides: Investigation and Mitigation, Transportation Research Board Special Report No. 247, pp. 129–177.

Tangestani, M.H., 2004. Landslide susceptibility mapping using the fuzzy gamma approach in a GIS, Kakan catchments area, SW Iran. Australian Journal of Earth Sciences 51, 439–450.

Temesgen, B., Mohammed, M.U., Korme, T., 2001. Natural hazard assessment using GIS and Remote Sensing Methods, with particular reference to the landslides in the Wondogenet area, Ethiopia. Physics and Chemistry of the Earth (C) 26 (9), 665–675.

Van Lynden, G.W.J., Mantel, S., 2001. The role of GIS and remote sensing in land degradation assessment and conservation mapping: some user experiences and expectations. International Journal of Applied Earth Observation and Geoinformation 3 (1), 61–68.

Van Westen, C.J., 1993. Gissiz, training package for Geographic Information Systems in Slope Instability Zonation, ITC—Pub.N. 15, Part 1 Enschede, The Netherlands, p. 245.

Van Westen, C.J., Seijmonsbergen, A.C., Mantovani, F., 1999. Comparing landslide hazard maps. Natural Hazards 20, 137–158.

Van Westen, C.J., Rengers, N., Terlien, M.T.J., Soeters, R., 1997. Prediction of the occurrence of slope instability phenomena through GIS-based hazard zonation. Geol Rundsch 86, 404–414.

Van Westen, C.J., Soeters, R., Sijimons, K., 2000. Digital geomorphological landslide hazard mapping of the Alpago area, Italy. International Journal of Applied Earth Observation and Geoinformation 2 (1), 51–60.

Varnes, D.J., 1978. Slope movement types and processes. In: Schuster, R.L., Krizek, R.J. (Eds.), Landslides: Analysis and Control. Transportation Research Board, National Academies of Science, Washington, DC, pp. 11–33.

Wright, D.F., Bonham-Carter, G.F., 1996. VHMS favourability mapping with GIS-based integration models, Chisel Lake-Anderson Lake area, In: Bonham-Carter, Galley, Hall (Eds.), EXTECHI: A Multidisciplinary Approach to Massive Sulfide Research in the Rusty Lake-Snow Lake greenstone belts, Manitoba. Geological Survey of Canada, Bulletin 426, pp. 339–376.

Xu, L., Krzyzak, A., Suen, C., 1992. Methods of combining multiple classifiers and their applications to handwriting recognition. IEEE Transactions on Systems, Man and Cybernetics 22, 418–435.

Yalcin, A., 2008. GIS-based landslide susceptibility mapping using analytical hierarchy process and bivariate statistics in Ardesen (Turkey): Comparisons of results and confirmations. Catena 72, 1–12.

Yamada, K., 2008. A new combination of evidence based on compromise. Fuzzy Sets and Systems 159 (2008), 1689–1708.

Zadeh, L.A., 1965. Fuzzy sets. IEEE information and control 8, 338–353.

Zadeh L.A., 1979. On the Validity of Dempster's rule of Combination of Evidence, Memo M79/24, University of California, Berkeley, USA.

Zolfaghari, A., Heath, A.C., 2008. A GIS application for assessing landslide hazard over a large area. Computers and Geotechnics 35, 278–285.